

The role of thermal contribution in the design of AA2024 Friction Stir Welded butt and lap joints: mechanical properties and energy demand

Davide Campanella^{1*}, Giulia Marcon¹, Alberto Lombardo¹, Gianluca Buffa¹
and Livan Fratini¹

^{1*}Department of Engineering, University of Palermo, viale delle Scienze, Palermo, 90128, Italy.

*Corresponding author(s). E-mail(s): davide.campanella@unipa.it;

Abstract

Although in recent times the use of solid-state welding processes as Friction Stir Welding (FSW) has become increasingly widespread, for some joint morphologies, as lap joints, there are still significantly less data available on both process parameters optimization and energy consumption. In the present paper, the authors investigated the possibility of enhancing the joint quality in two different configurations, i.e. Lap and Butt joints, taking into account Specific Thermal Contribution (STC) conferred to the weld. Strength, micro-hardness and microstructure were evaluated on the produced AA2024 aluminum alloys butt and lap joints. The Surface Response Method (RSM) was used to investigate the effects of the main process parameters and to identify optimal technological parameters in terms of joint resistance, while the Specific Energy Consumption (SEC) of the entire process was acquired with the aim to provide design guidelines taking into account, at the same time, mechanical performance and environmental impact. It was found that the same optimal range of revolutionary pitch can be identified for both the configurations. Additionally, maximizing welding speed, for a given revolutionary pitch, contributes to significantly reduce the environmental impact of the process with no detrimental effect on the joint performance.

Keywords: Friction Stir Welding (FSW), Response-Surface Methodology (RSM), Specific Thermal Contribution (STC), Specific Energy Consumption (SEC)

1 Introduction

Friction Stir Welding (FSW), developed by the Welding Institute of Cambridge in 1991 [1], is currently considered as one of the best performing processes for the production of aluminum alloy joints.

In this solid-state welding process, the heat and plastic deformation induced by the rotational and translational motion of a non-consumable tool are

used to create the joint, as the FSW welding formation mechanism can be assimilated to extrusion and forging of the plates to be welded. Most of the deformation is caused by the stirring action exerted by the tool pin on the pieces. Due to the rotation, the metal that is in contact with the pin is extruded and immediately forged through the passage of the tool shoulder.

Friction stir welding has been studied intensively

in recent years due to its importance for key industrial applications in the aeronautical, aerospace and ground transportation industries [2], [3]. Initially, this process was mainly applied for the production of butt joints and the majority of the studies were based on this joint configuration, while friction stir lap welding received considerably less attention [4]. However, it has been demonstrated that FSW can be effectively applied to a variety of joints designs as lap joints, T joints, butt joints and even fillet joints [1]. The wide use of FSW in lap joint configuration would significantly expand the possible applications in several fields, as aircraft and naval structures as the FSW of lap joints may substitute other joining processes like spot welding or riveting.

The mechanical properties of a FSWed joint (butt and lap-joint configurations) depend on various factors. These factors include the welding process parameters (tool rotational speed, tool traverse speed, tool tilt angle, etc.), base material, tool geometry (pin and shoulder size, pin profile, etc.) and tool material, and environment conditions (submerged, non-submerged, heat-assisted tooling, cooling-assisted tooling) [5]. Because of the dependence on several parameters, it is difficult to optimize the welding conditions to obtain a high-quality weld joint with superior mechanical properties. General guidelines can be established by reviewing the available literature.

Different studies have been focused on the statistical analysis, e.g. analysis of variance (ANOVA), for determining the most significant parameters that affect the weld joint mechanical properties. Apart from mechanical property optimization-based studies, the statistical-based models can also be used for weld quality assessment [6] and monitoring, as well as early prediction of weld defects. Sabry et al. [7] developed a new method for predicting discontinuity formation, its position and magnitude during aluminium alloy (AA6061) friction stir welding of butt joints. The effectiveness of the technique was demonstrated using visual inspection, hardness and tensile tests. The measured current was analyzed through power calculations. In each of the FSW stages, the energy consumption significantly varied, clearly distinguishing the penetration of the tool, its revolution, its traverse movement and its metal removal rate. Instead of focusing on the

analysis of variance (ANOVA) which checks the adequacy of the developed mathematical model by 95% confidence levels, Response surface methodology (RSM) was employed to develop a statistical model for each joint configuration. Moreover, tensile and hardness tests also showed that welds at high power usage failed continuously within the welding area, due to reduced welding temperature and absence of penetration in the welding zone.

Vahdati et al. [8] carried out a statistical analysis and optimization of the yield strength and tensile strength of Al7075 butt joints produced by FSW and SFSW using response surface methodology and desirability approach. The results show that the first order parameter referring to the tool rotational speed, the interactional term obtained combining the tool rotational speed and the tool shoulder diameter, and the second order term obtained from the square of the tool rotational speed are the most important terms affecting the yield strength of the joints. In addition, the first order parameter of the tool rotational speed and the second-order term of the square of the tool rotational speed have been identified as the most important terms affecting the ultimate tensile strength of the FSW joints. Viscusi et al. [9] examined the strength of FSW aluminum alloy lap joints in two different welding zones, i.e. Heat Affected Zone and nugget. The authors used central factorial design, response surface methods and gradient algorithms in order to achieve the process parameters optimization.

In recent years, a strong trend towards environmentally benign manufacturing has been emerging, mainly owing to more stringent regulations and competitive economic advantages [10]. However, discrete part manufacturing processes are still not well documented in terms of their environmental impact [11]. Consequently, environmental optimization measures are often not sufficiently pursued and improved machine tool design, in terms of ecological footprint reduction, has only been targeted for a few common processes. Furthermore, the current trend of employment of more energy-intensive processes is expected to increase the environmental impact of manufacturing [12]. FSW has been receiving growing interest also owing to its energy efficiency, environment friendliness and versatility that makes it a promising ecologic and “green” technology [13]. It is thought that friction stir welding consumes less

energy as compared to the fusion welding technologies, due to the lower temperatures involved and the solid-state nature of the process. Furthermore, FSW leads to a decrease in material waste and allows the user to avoid radiation and dangerous fumes.

Bevilacqua et al. [14] have shown that the environmental impact of butt joints friction stir welding is strongly affected by rotational and welding speeds. The environmental impact was also related to the mechanical properties of joints, expressed as ultimate tensile strength and ultimate elongation. The influence of tool rotation and feed rate on butt joints energy consumption was investigated by some of the authors [15], highlighting the contribution of the main sub-units thus determining the total demand by a power study, with breakdown analysis.

From the literature analysis, two main factors arise: (i) there is significantly less knowledge on the process parameters optimization and energy consumption for lap joints with respect to butt joints; (ii) although mechanical properties and environmental impact have been studied, they have not been taken into account simultaneously, together with the joint morphology, for the process parameters choice. Often process designer have the possibility to select the most appropriate joint morphology for a given application, while modern requirements impose to reach high mechanical efficiency and low environmental impact. In this paper, the authors carried out an experimental study focused on FSW of butt and lap joints made out of AA2024-O aluminum alloy sheets with the aim to provide design guidelines helping process engineers in the selection of the optimal joint configuration for a given application. The welded joints were subjected to tensile tests, micro hardness tests as well as metallographic analysis. Specific Energy Consumption (SEC), was also acquired and the Surface Response Method (RSM) was used to investigate the effect of the main process parameters and to identify optimal technological parameters in terms of mechanical performance and energy consumption of the weld.

2 Experimental procedures

2.1 Welding tests

The FSW experimental tests were carried out using AA2024-O aluminum alloy sheets having thickness of 2.7 mm. Table 1 reports the main mechanical properties of the considered material. The specimens were welded using an ESAB

Table 1: Main mechanical properties of the examined AA2024 alloy

Ultimate Tensile Strength [MPa]	Yield Strength 0.2% Proof [MPa]	Shear Strength [MPa]	Vickers Hardness [HV]
192 (± 3.9)	75.8	124 (± 3.2)	65

LEGIO machine (Figure 1a).

In order to ensure uniform welding conditions along the weld seam, stirring head force control was set on the machine. For all the tests, constant tool tilt angle of $2.5^\circ(\theta)$ and tool plunge of 2.9 mm and 2.5 mm for the lap and butt configurations, respectively, were assigned. The tool plunge speed was fixed to 0.1 mm/sec and the dwell time was equal to zero for all tests. While in the butt joint configuration the sheets were fixed in mutual contact along the thickness, an overlapping between the sheets of 20 mm was given in the lap joint configuration.

H13 steel, quenched at 1020 °C, characterized by a 52 HRC hardness, was selected as the tool material for the experimental tests. Cylindrical screw pins (Figure 1b) were used with the geometrical characteristics reported in Table 2.

Table 2: Geometries of the utilized H13 tool

Joint configuration	Butt	Lap
Shoulder diameter [mm]	10	10
Pin diameter [mm]	4	4
Pin height [mm]	2.4	2.7

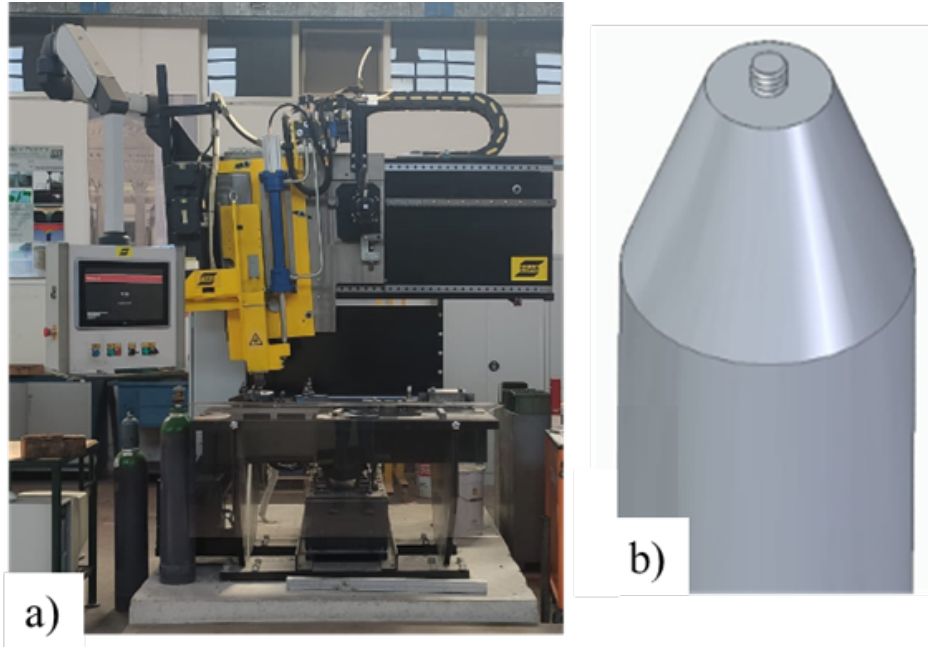


Fig. 1: a) ESAB Legio machine; b) sketch of the screwed pin tool

2.2 Statistical methodology

As far as the process parameters were concerned, the tool rotation and the feed rate were varied from 800 rpm up to 1200 rpm and from 10 mm/min up to 120 mm/min, respectively. The detailed list of values used for the different sets is reported in Table 3. The same values were used for both butt and lap configurations. In

Table 3: Variables considered for butt and lap joint configurations

Process Variable	Investigated values
Rotational speed [rpm]	800, 1000, 1200
Feed rate [mm/min]	10, 20, 30, 40, 45, 50, 60, 120

order to detect the best welding performance, as a function of feed rate (Fr) and rotational speed (Rs), the Response-Surface Methodology (RSM), which comprises a set of methods for exploring for optimum operating conditions through experimental methods, was considered [16]. In particular, this method involves the carry out of several experiments and the use of the results of

one experiment to provide direction for what to do next. The initial parameters taken into account in this study derive from a research published by Wang et. al [17]. The fundamental methods imply the assignment of first order (linear) or second order (quadratic) functions of the predictors of the response variable.

Statistical analyses were carried out by means of multivariate linear regression methodologies, for example

$$y_i = \beta_0 + \beta_1 x_{1i} + \beta_2 x_{2i} + \beta_{12} x_{1i} \cdot x_{2i} + \beta_3 x_{1i}^2 + \epsilon_i \quad (1)$$

where, for $i = 1, \dots, n$ observations, y_i is the dependent variable, x_i are any explanatory variables, including quadratic terms (x_i^2) and two-way interactions ($x_{1i}x_{2i}$), and ϵ_i is the error term. Finally, in order to detect the most performing model, stepwise model selection was explored where several multiple linear regression models with different predictors were sequentially compared, improving iteratively a performance measure. In particular, stepwise model selection typically uses as measure of performance an information criterion, which balances the fitness of a model with the number of predictors employed.

One of the common criteria is the Bayesian Information Criterion (BIC):

$$\text{BIC}(\text{model}) = -2 \ell(\mathbf{x}; \beta) + k \ln(n) \quad (2)$$

where $\ell(\mathbf{x}; \beta)$ is the log-likelihood of the model considering the vector of the covariates \mathbf{x} (how well the model fits the data) and k is the number of parameters considered in the model (how complex the model is).

Each test was repeated seven times and, in order to test the quality of the weld, micro-observations were carried out. Tensile tests and shear tests were carried out, for butt and lap configuration, respectively, on a Galdabini Quasar 600 for all the process conditions. Macro observations were performed to analyze the material area involved in the process mechanics and identify possible macro-defects. In order to attain these results, the specimens were resin casted, polished and finally acid-etched with the Keller reagent and before being observed through an Olympus GX51 Optical Microscope. Additionally, Phenom ProX Desktop was used for the SEM analyses.

2.3 Energy consumption analysis

During the welding tests, the power consumption was acquired using a Cauvin Arnoux C.A 8331 multimeter **with accuracy corresponding to $\pm (0.5\% + 200 \text{ mV})$** . For every test, the power profile corresponding to the chosen technological parameters was recorded. Figure 2 shows the multimeter connected to the main supply of the FSW machine during the tests. The considered measuring time covered the interval from the machine start-up until the tool lift. The utilized energy was calculated by multiplying the supplied power by the duration of the given operation. Studying the power consumption enabled the quantification of the energy shares of different production modes, and thus, the most power-consuming phase was also identified.

3 Results and Discussions

The obtained results are divided into three subsections. In the first two, the mechanical properties and the energy demands, respectively, are presented as a function of the used process parameters, while in the last a combined analysis is

shown with the aim to help process designers in the choice of proper condition for a given application.

3.1 Mechanical characterization

First, all the produced joints cross sections were observed in order to determine the presence of flow defects. For all the process conditions investigated, no defect was observed. For sake of simplicity, the joints obtained with three different combinations of process parameters are shown, for the two configurations analyzed, in Figure 3. After macro-observations, the micro-hardness in the transverse section of the welded joints was investigated. In Figure 4 the micro-hardness values (HV) obtained at mid-thickness of the cross section of the three butt joints shown in the previous figure are shown.

It can be observed that, for all the tests reported, a significant local hardening of the material occurs in the stirred zone mainly due to the dynamic recrystallization resulting in finer grain size. It is worth noting the considered alloy is in the O state, hence no loss of the hardness due to the temper takes place. Additionally, the thermal cycle that the material experience due to the process, can favor the presence of precipitates contributing the HV increase.

In order to better understand such material hardening phenomenon, the Cu precipitation density in the weld nugget was investigated. From Figure 5, it can be observed that in the nugget zone, the dispersion of Cu particles was higher compared to the Heat Affected Zone thus conferring higher local hardness, being the cluster sizes observed in HAZ and nugget $14 \mu\text{m}$ and $7 \mu\text{m}$, respectively. In Figure 6 the hardness values relative to the lap joints are shown. A vertical line across the two sheets, in the weld center, was considered. It is possible to note that in the area closer to the joint top surface the hardness is higher due to the maximum stirring of the material with respect to that in the pin area. However, in the pin area material hardening was reached anyway, even though the measured hardness values were lower. In FSW, the process parameters having a stronger influence on the mechanical properties of the joint are rotation speed (Rs) and tool feed rate (Fr). In particular, these two parameters determine the specific heat input to the joint. For this reason, a

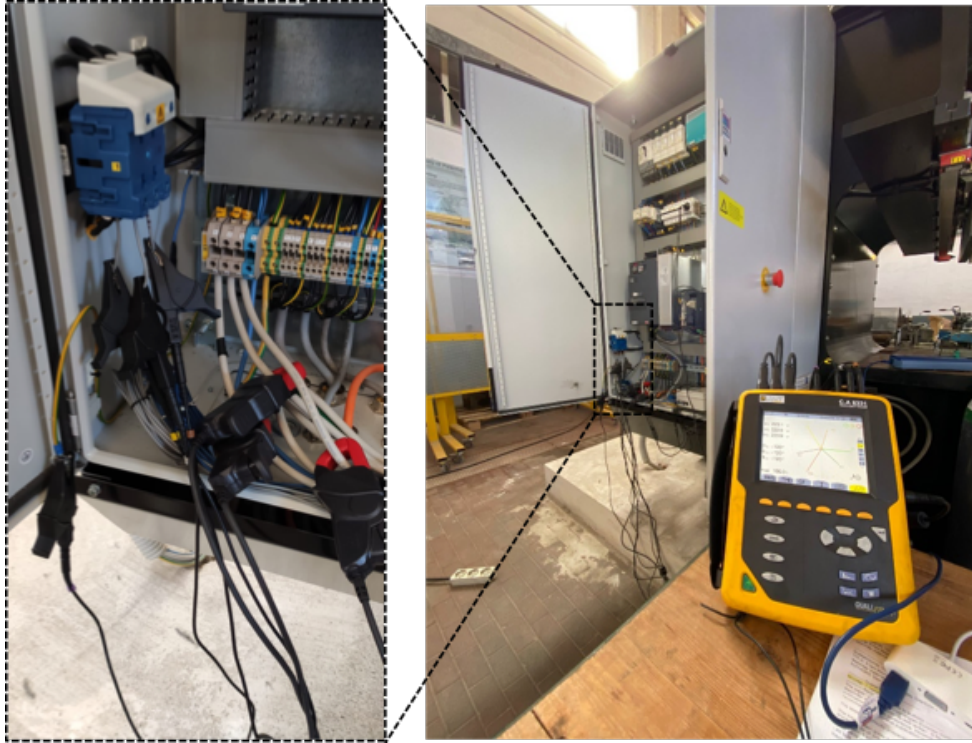


Fig. 2: Cauvin Arnoux C.A 8331 used during the tests

unique process parameter more closely representing the conferred heat was utilized, namely the revolutionary pitch, defined as the ratio between the tool feed rate and the tool speed rotation:

$$Rp = \frac{Fr}{Rs} \left[\frac{mm}{rpm} \right] \quad (3)$$

Table 4 collects the **average** values obtained from the tests concerning from different configurations of the parameters.

After collecting all the data, referring to the parameters presented in Table 4, the influence of each variable was investigated with the aim to identify the relationship among all these variables. Multiple regression is a statistical method that allows the study of the relationship between a single dependent variable (UTS o Shear force for butt and lap, respectively) and several independent variables (Rp, Fr, Rs). The aim of the study is to detect whether any particular independent variable affects the dependent variable and to estimate the magnitude of this effect, if any.

Following the stepwise approach previously introduced, the best models in terms of model fitting include all independent variables revolutionary

pitch (Rp), feed rate (Fr) and rotational speed (Rs) and the corresponding quadratic terms and two-way interactions. The equations estimated are the following:

$$\begin{aligned} UTS = & -1.26e^{02} + 1.05e^{04}Rp - 5.63Fr \\ & + 2.94e^{-01}Rs - 8.26e^{04}Rp^2 + 9.22e^{-02}Fr^2 \\ & - 4.49e^{-03}Fr \cdot Rs - 1.76Rp^2 \cdot Fr^2 \end{aligned} \quad (4)$$

$$\begin{aligned} SF = & -1.61e^{04} + 7.74e^{05}Rp - 1.63e^{03}Fr \\ & + 3.49e^{01}Rs - 8.39e^{06}Rp^2 - 9.98Fr^2 \\ & - 1.87e^{-02}Rs^2 + 1.78e^{04}Rp \cdot Fr \\ & + 8.89e^{-01}Fr \cdot Rs + 4.42e^{01}Rp^2 \cdot Fr^2 \end{aligned} \quad (5)$$

where the corresponding adjusted- R^2 are equal to 0.51 and 0.80, and the BIC values equal to 470.67 and 341.34, respectively. Although the goodness of fit of both models is sufficiently high, the interpretation of such relations can be extremely difficult. A graphical representation is provided in Figure 7. For this reason, simplified models are proposed

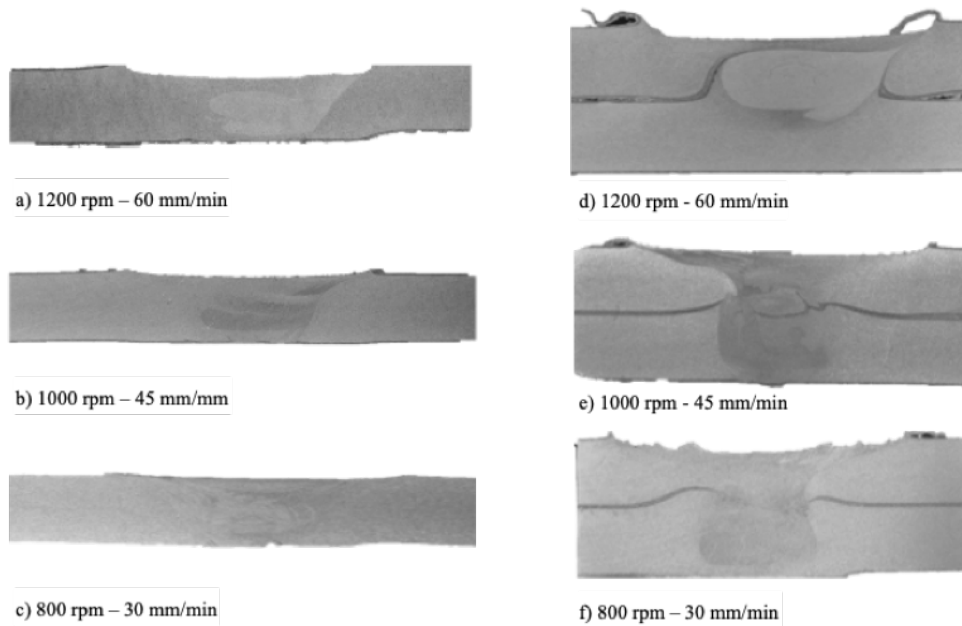


Fig. 3: Macro observations of cross sections on (a, b, c) butt and (d, e, f) lap joints

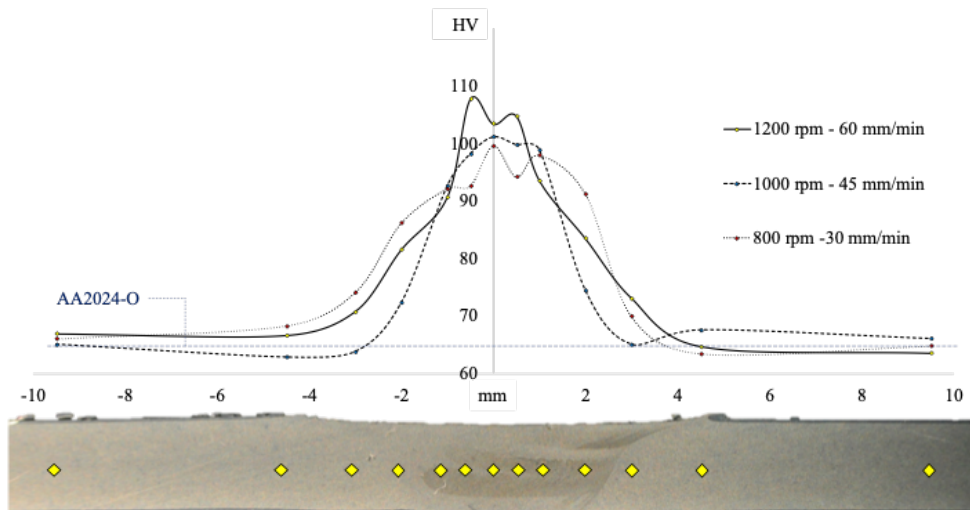


Fig. 4: Vickers hardness on butt joint

which only depend on the heat input in terms of revolutionary pitch.

The obtained models are the following:

$$UTS = 152.37 + 1585.98Rp - 13725.80Rp^2 \quad (6)$$

$$SF = 276.57 + 6230.08Rp - 51342.54Rp^2 \quad (7)$$

where both UTS and Shear Force (SF) are modeled through a function of revolutionary pitch

(Rp). Both models still explain significantly the variability through the linear and quadratic form of revolutionary pitch although the model-fitting in terms of adjusted- R^2 reduced (0.11, and 0.15 respectively). Both models are represented in Figure 8.

In order to compare the equations for butt and lap joints and provide 90 % confidence bands, the

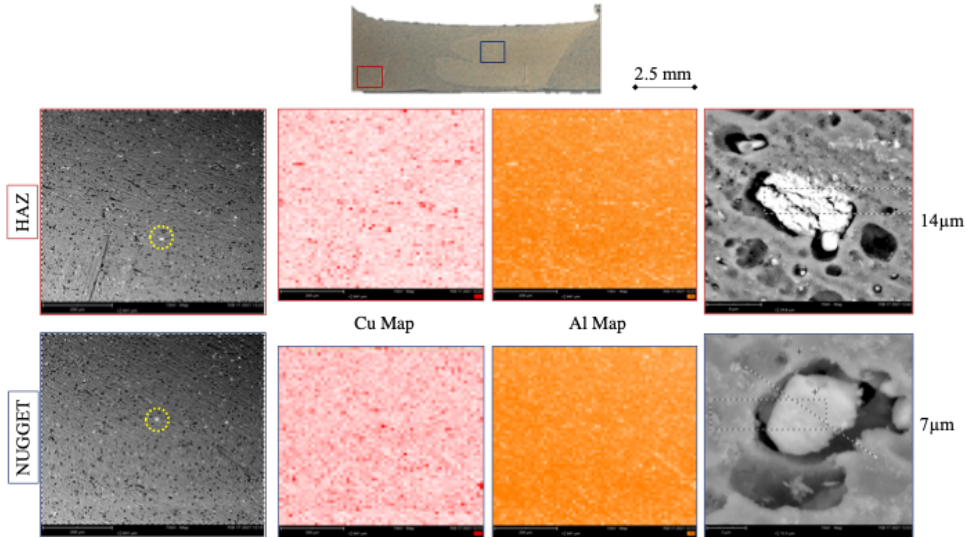


Fig. 5: SEM analysis on the test characterized by 1200 rpm 60 mm/min

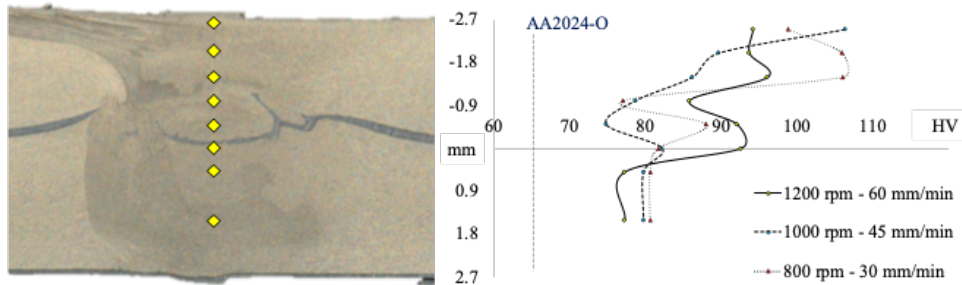


Fig. 6: Vickers hardness on lap joint

results are jointly represented in Figure 9.

It could be observed that for a range of revolutionary pitch between 0.045 and 0.06 a high-performance joint was observed for the two configurations whereas, outside the above-mentioned range, the mechanical performance decreases. Table 5 shows the confidence bands (90%) for both models, in correspondence of the central values of revolutionary pitch, which provides a representation of the uncertainty about the regression model where the greatest values of the response variable are observed.

3.2 Energy demand characterization

A typical power profile obtained during the FSW process is shown in Figure 10. It can be observed

that almost 100 seconds were necessary for the activation of auxiliary modules and 50 seconds for tool positioning in the starting position. After about 200 seconds, a high peak was observed due to the contact of the tool with the sheets. This occurs since the material is still cold and a high force is required for the tool penetration. After the plunge phase, a steady state power is measured, corresponding to the actual welding phase, before tool lift.

The Specific Thermal Consumption (STC) was selected in order to compare the two joint configurations. For each test, the power profile was acquired and the STC was calculated as the ratio between the power used for the weld and the tool feed rate.

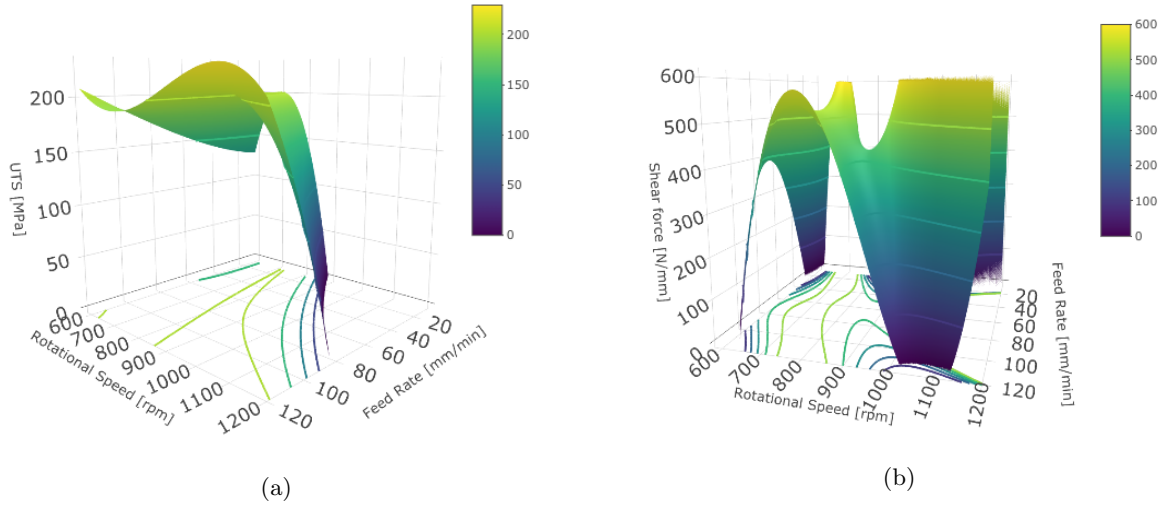


Fig. 7: UTS and Shear Force plots vs. Feed rate and Rotational speed, referring to models (4) and (5).

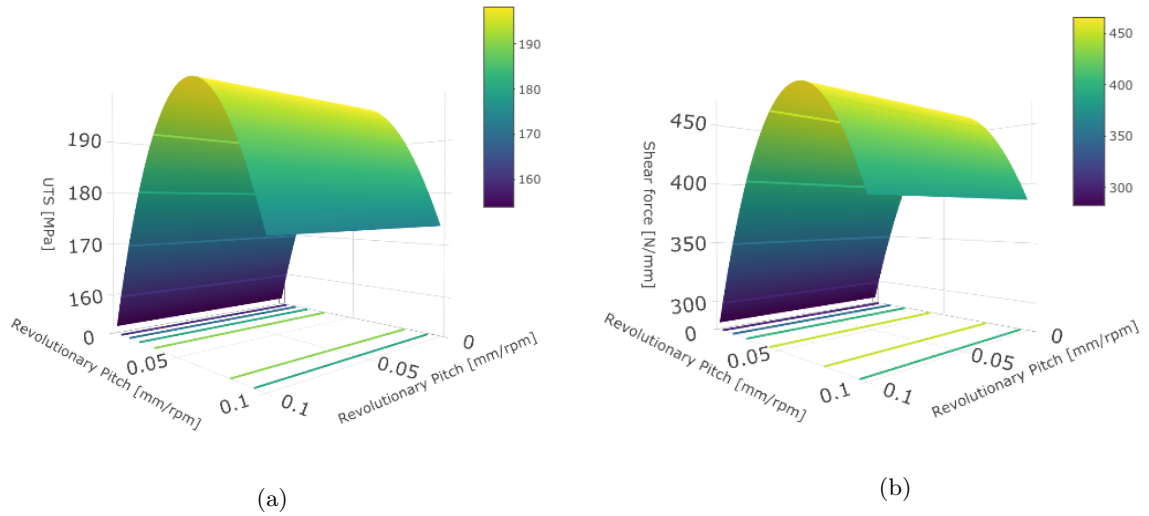


Fig. 8: UTS and Shear Force plots vs. Revolutionary pitch, referring to models (6) and (7)

$$STC = \frac{P_{FSW} - P_0}{Fr} \left[\frac{J}{mm} \right] \quad (8)$$

The power required by the weld is mainly due to the friction forces work and the material deformation dissipated into heat. Since a direct evaluation of the power input in each weld was not possible,

an indirect measurement was adopted, i.e., the difference between the electrical power consumed by the ESAB machine during the test (P_{FSW}) and the one consumed in the no tool penetration conditions (P_0) were used for the power calculation. It is worth noting that for the STC calculation the power value used accounted for just the welding phase i.e., when the power reaches a steady state, thus avoiding the transient phase due to auxiliary

Table 4: Joint resistance (\pm standard deviation) obtained for butt and lap joints

		Joint configurations		
		Butt	Lap	
Technological Parameters [mm/min - rpm]	Rev. Pitch [mm/rpm]	UTS [MPa]	Shear force [N/mm]	
10	800	0.008	159 (± 7.1)	335 (± 16.3)
	1000	0.010	153 (± 5.2)	322 (± 15.6)
	1200	0.013	194 (± 2.3)	162 (± 14.7)
20	800	0.017	168 (± 6.7)	358 (± 3.4)
	1000	0.020	119 (± 8.1)	491 (± 6.5)
	1200	0.025	176 (± 6.2)	379 (± 4.2)
30	800	0.025	192 (± 6.6)	525 (± 4.1)
	1000	0.030	188 (± 5.2)	287 (± 4.8)
	1200	0.038	182 (± 16.2)	442 (± 5.1)
40	800	0.033	188 (± 18.4)	399 (± 4.3)
	1000	0.040	188 (± 11.2)	414 (± 6.2)
	1200	0.050	194 (± 7.1)	435 (± 6.9)
45	800	0.038	196 (± 12.2)	463 (± 4.5)
	1000	0.045	196 (± 5.7)	476 (± 10.1)
	1200	0.056	192 (± 12.3)	318 (± 8.2)
50	800	0.042	190 (± 6.6)	417 (± 5.2)
	1000	0.050	217 (± 5.2)	435 (± 6.1)
	1200	0.063	199 (± 2.9)	459 (± 4.2)
60	800	0.050	179 (± 5.2)	403 (± 6.5)
	1000	0.060	188 (± 12.7)	424 (± 7.6)
	1200	0.075	204 (± 14.3)	432 (± 7.4)
120	800	0.100	199 (± 10.4)	234 (± 11.1)
	1000	0.120	190 (± 12.2)	328 (± 12.7)
	1200	0.150	163 (± 14.7)	398 (± 13.1)

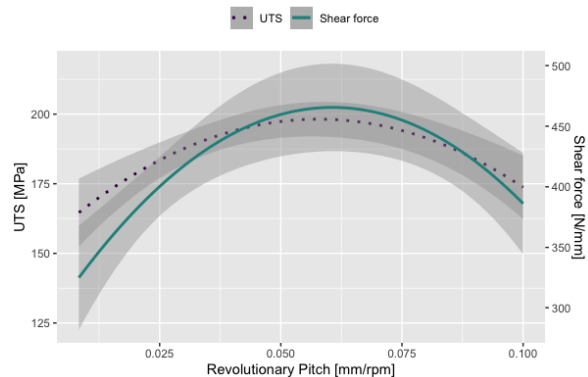
devices activation (e.g. hydraulic pump for force control) or tool pre-welding movements.

In Table 6 the STC values obtained from all the tests carried out are reported. From the data shown in Table 6 it can be observed that P_0 decreases with increasing rotational speed. This could be explained considering that inertial forces, at higher rpm, help in overcoming the frictional forces present in the machine.

Equations (9) and (10) describe the STC trends lines for the Butt and Lap case studies, respectively, analyzed as a function of revolutionary pitch (Rp):

$$STC_{Butt} = 2628.16 - 69535.74Rp + 739499.94Rp^2 \quad (9)$$

$$STC_{Lap} = 7966.91 - 269435.89Rp + 2907602.25Rp^2 \quad (10)$$

**Fig. 9:** UTS in primary y-axis (dotted line) and Shear Force in secondary y-axis (solid line) vs. Revolutionary pitch**Table 5:** 90% Confidence Bands of quadratic models (6) and (7).

	Joint configurations			
	Butt UTS [MPa]	Lap Shear Force [N/mm]		
Rev. Pitch [mm/rpm]	Lower bound	Upper bound	Lower bound	Upper bound
0.045	190.35	201.55	420.30	485.62
0.050	191.51	203.21	425.16	494.28
0.055	192.01	204.15	428.19	499.64
0.060	191.88	204.36	429.43	501.66

Such models are a good trade-off between model performance and complexity. The corresponding adjusted- R^2 are equal to 0.92 and 0.94, respectively.

Figure 11 shows the polynomial regression describing the STC trend as a function of revolutionary pitch for the two analyzed configurations. It can be seen that for both the configurations a minimum is found. This occurs because for too low values of the revolutionary pitch the disadvantages related to the high power required to maintain high tool rotation overshadows the advantages due to the lower material resistance because of the increased welding temperature, as demonstrated by some of the authors in previous research [15]. On the other hand, for high values of the revolutionary pitch the material does not reach a proper softening state, offering a high resistance to the

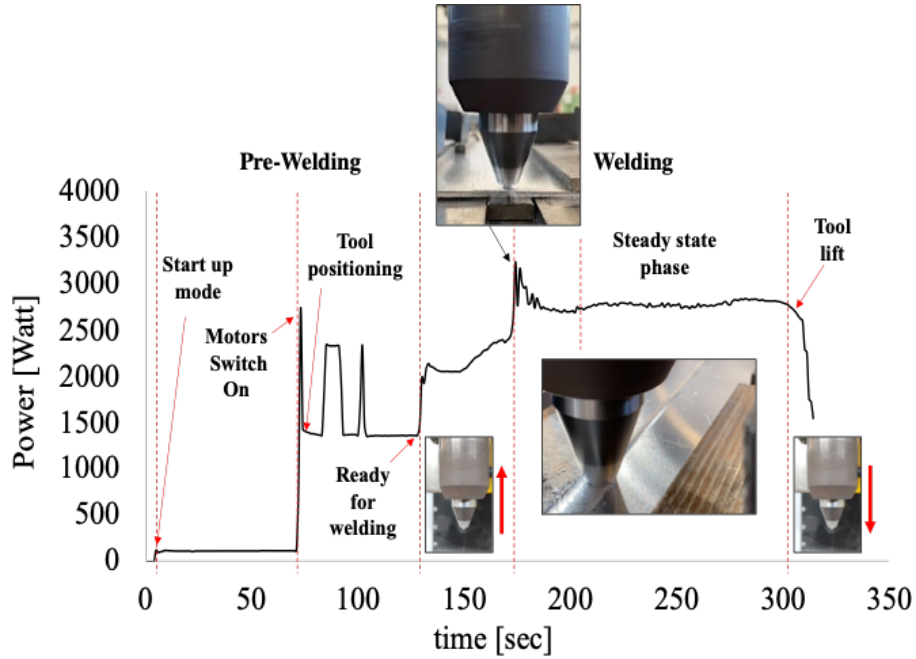


Fig. 10: Power profile in FSW process, 1000 rpm and 50 mm/min, butt joint case study

moving tool both in terms of torque and advancing resistance, thus requiring higher power.

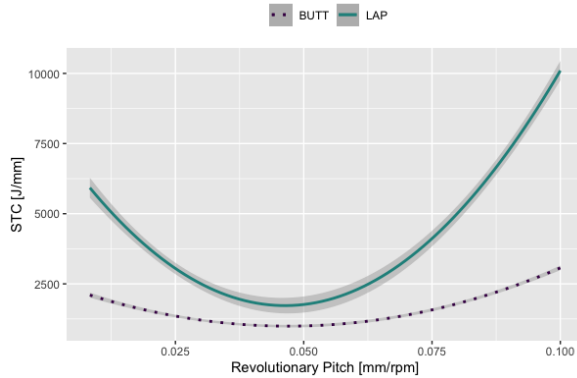


Fig. 11: Comparison of STC vs Revolutionary pitch in the butt and lap configurations

It is worth noting that butt joints overall show lower values of STC even if the tools had the same shoulder diameter. This is due to the fact that the tool penetration values were different, being 0.2 mm higher in the case of Lap joints as, for this configuration, the selected tool depth was necessary to reach the sheets interface.

3.3 Combined analysis

In order to better compare the approaches proposed the mechanical performance parameter measured (UTS and shear force for butt and lap, respectively) and the STC have been plotted (Figure 12). It is noted that, for both the joint configurations, an optimal range of revolutionary pitch exists, within which minimum STC and maximum resistance are found. Additionally, the same RP interval can be identified for both butt and lap joints. For such intervals, the 90% confidence bands of STC models, referring to eq.(9) and eq.(10), are reported in Table 7. In order to assess the environmental impact of the FSW process in terms of energy consumption, the Specific Energy Consumption (SEC) was considered [18]. Even if the SEC value has the same unit of measurement as that of the STC, it has a different calculation method as reported in equation 11.

$$SEC = \frac{P_{FSW} \cdot t}{l} \quad \left[\frac{J}{mm} \right] \quad (11)$$

In fact, the SEC parameter is directly proportional to the power required for the process (P_{FSW}) and the tool operation time (t) while it is inversely proportional to the weld length (l) [18]. Three process

Table 6: STC values obtained in butt and lap joints

Technological Parameters [mm/min - rpm]		Joint configurations				
		Butt			Lap	
		P_0 [W]	P_{FSW} [W]	STC [J/mm]	P_{FSW} [W]	STC [J/mm]
10	800	2239	2591	2114	3161	5532
	1000	2216	2559	2059	3107	5347
	1200	2170	2492	1929	2988	4905
20	800	2128	2722	1782	3598	4410
	1000	2105	2668	1690	3472	4102
	1200	2068	2575	1522	3247	3538
30	800	2100	2860	1520	3875	3549
	1000	2042	2771	1458	3594	3103
	1200	2004	2604	1200	3887	2825
40	800	2025	2895	1305	3266	2482
	1000	1996	2769	1159	3824	2437
	1200	1962	2626	996	3529	2351
45	800	2004	2904	1200	3862	2230
	1000	1977	2775	1064	3515	2051
	1200	1944	2643	932	3175	1846
50	800	1986	2920	1121	3504	1821
	1000	1962	2792	996	3782	1820
	1200	1925	2663	886	3171	1661
60	800	1962	2958	996	3550	1588
	1000	1931	2830	899	3229	1557
	1200	1898	2790	892	3515	1617
120	800	1853	4281	1214	7901	3024
	1000	1825	5391	1183	7271	5223
	1200	1790	8092	1051	7536	8373

conditions corresponding to fixed revolutionary pitch equal to 0.05 mm/rpm (i.e. within the optimal range identified, see again Figure 12) were considered. Besides the process conditions characterized by tool rotation of 1200 rpm and feed rate of 60 mm/min, two additional case studies were then investigated, characterized by the same revolutionary pitch. For these two process conditions, tool rotation and feed rate were obtained multiplying and dividing by two, respectively, the tool rotation and feed rate of the 1200 rpm - 60

mm/min reference case study. Table 8 shows the parameters investigated and the SEC values calculated for all the three cases considered. Figure 13 shows the UTS (in the primary y-axis) and SEC (in the secondary y-axis) values as a function of feed rate. It is worth noting that the feed rate has a significant impact on the energy consumption of the process, as it directly determines, for a given weld length, the duration of the process itself. From Figure 13, it can be observed that the mechanical performances of the joints

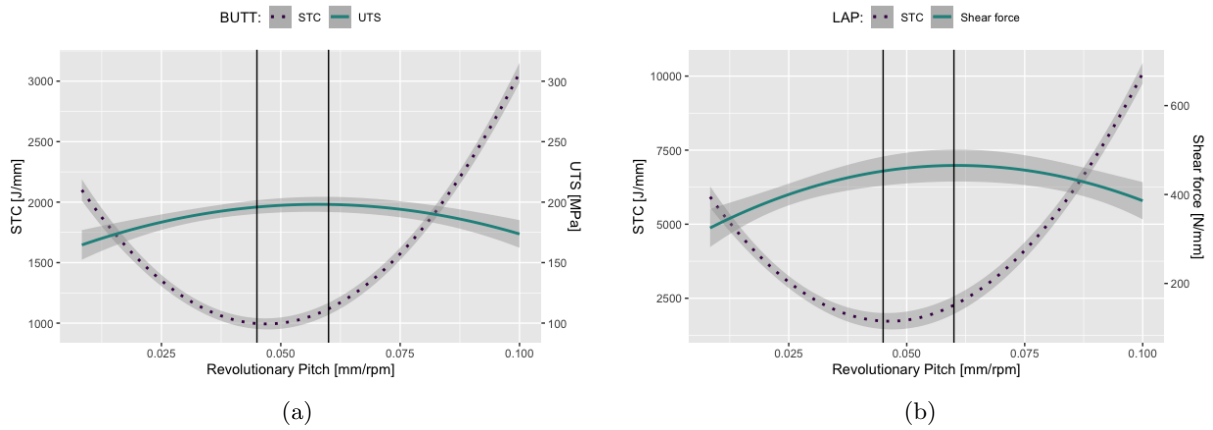


Fig. 12: Comparison of STC and mechanical performance vs Revolutionary pitch in the butt and lap configurations with 90% confidence bands

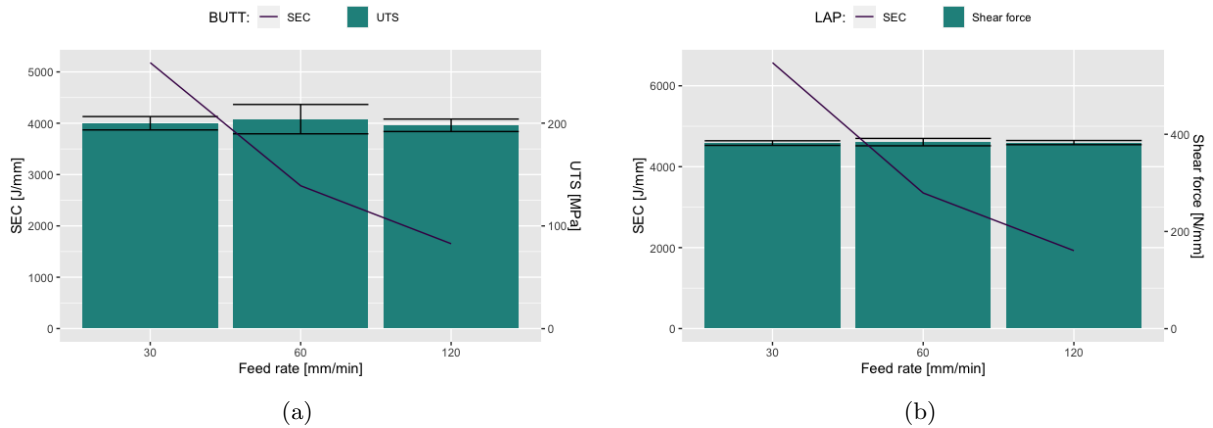


Fig. 13: Mechanical Performances and energies comparison for a) butt and b) lap joints with constant revolutionary pitch

are almost constant for the selected revolutionary pitch, although obtained with tool rotation and feed rate values varying in a quite large range. In turn, the measured SEC shows a decreasing trend with increasing feed rate. In this way, it can be stated that in the design of the FSW process, once identified the revolutionary pitch resulting in optimal mechanical performances, the environmental impact can be minimized by maximizing, depending on the used machine limits, the feed rate.

4 Conclusion

The presented research article reports the results of an experimental analysis on the FSW of AA2024-O butt and lap joints. Based on the obtained results the following conclusions can be drawn:

- Several process parameters affect the process mechanics and consequently, the joint resistance. The Specific Thermal Contribution can be assumed as a key process parameter to be utilized for the overall designing of the FSW process resulting from a strong dependence of STC on the revolutionary pitch, i.e. the ratio

Table 7: 90% Confidence Bands of quadratic models (9) and (10)

Rev. Pitch [mm/rpm]	Joint configurations			
	Butt STC [J/mm]		Lap STC [J/mm]	
	Lower bound	Upper bound	Lower bound	Upper bound
0.045	951.82	1041.26	1458.91	2001.47
0.050	953.26	1046.98	1477.06	2051.18
0.055	992.13	1089.24	1646.69	2240.18
0.060	1068.59	1167.84	1968.14	2568.11

Table 8: Revolutionary pitch 0.05 mm/rpm constant for butt and lap joint configurations

Butt	Rotational speed [rpm]	600	1200	2400
	Feed rate [mm/min]	30	60	120
	Rev. Pitch [mm/rpm]	0.05	0.05	0.05
	<i>SEC [J/mm]</i>	<i>5180</i>	<i>2782</i>	<i>1653</i>
	<i>Performance [MPa]</i>	<i>200</i>	<i>204</i>	<i>198</i>
Lap	Rotational speed [rpm]	500	1000	2000
	Feed rate [mm/min]	30	60	120
	Rev. Pitch [mm/rpm]	0.06	0.06	0.06
	<i>SEC [J/mm]</i>	<i>6571</i>	<i>3351</i>	<i>1926</i>
	<i>Performance [N/mm]</i>	<i>382</i>	<i>384</i>	<i>383</i>

between feed rate and tool rotation is found. As for a given material and sheet thickness, the energy consumption of lap joints is larger than the one of butt joints. This is can be explained due to the larger tool plunge value needed in order to weld the sheets in lap configuration.

- The same “optimum” range of revolutionary pitch can be identified for maximizing joint’s strength and eventually, minimizing energy consumption for a given joint configuration. Additionally, the same range was identified also for the two configurations.
- When a proper value of revolutionary pitch, maximizing the joint mechanical performance, is identified, the combination of process parameters resulting in maximum feed rate should be chosen, depending on the welding machine limits, in order to minimize the environmental impact of the process.

These conclusions assist in the designing of experimental campaign in light of proper parameter

selection. Further research work on the studying of the effects of process parameters on working with sheets of varying thicknesses.

Declarations

- Ethical Approval the Authors Disclose potential conflicts of interest; also the research here presented does not involve either Human Participants or Animals.
- Consent to Participate: Not Applicable
- Consent to Publish: Not Applicable
- Authors Contributions:
Davide Campanella: Conceiving the idea, performing experimental, analysis of the results and draft writing.
Giulia Marcon: Conceiving the idea, analysis of the results and draft revision.
Gianluca Buffa: Draft revision and research coordination.
Alberto Lombardo: Research coordination.
Livan Fratini: Overall revision and research coordination.
- Funding: Not Applicable
- Competing Interests: The Authors disclose any financial and non-financial competing interests that could inappropriately influence, or be perceived to influence, this work.
- Availability of data and materials: Not Applicable

References

- [1] Mishra, R. S. & Ma, Z. Friction stir welding and processing. *Materials science and engineering: R: reports* **50** (1-2), 1–78 (2005) .
- [2] Celik, S. & Cakir, R. Effect of friction stir welding parameters on the mechanical and microstructure properties of the al-cu butt joint. *Metals* **6** (6), 133 (2016) .
- [3] Moreira, P., De Figueiredo, M. & De Castro, P. Fatigue behaviour of fsw and mig weldments for two aluminium alloys. *Theoretical and applied fracture mechanics* **48** (2), 169–177 (2007) .
- [4] Chen, Z. & Yazdanian, S. Friction stir lap welding: material flow, joint structure and

- strength. *Journal of Achievements in Materials and Manufacturing Engineering* **55** (2), 629–637 (2012) .
- [5] Buffa, G., Campanile, G., Fratini, L. & Prisco, A. Friction stir welding of lap joints: Influence of process parameters on the metallurgical and mechanical properties. *Materials Science and Engineering: A* **519** (1-2), 19–26 (2009) .
- [6] Mozumder, M. S., Mairpady, A. & Mourad, A.-H. I. *Hdpe/tio2 nanocomposite: Fabrication and optimization of mechanical property by rsm and ann*, Vol. 287, 54–58 (Trans Tech Publ, 2019).
- [7] Sabry, I., Gadallah, N. & Abu-Okail, M. *Optimization of friction stir welding parameters using response surface methodology*, Vol. 973, 012017 (IOP Publishing, 2020).
- [8] Vahdati, M., Moradi, M. & Shamsborhan, M. Modeling and optimization of the yield strength and tensile strength of al7075 butt joint produced by fsw and sfsf using rsm and desirability function method. *Transactions of the Indian Institute of Metals* **73** (10), 2587–2600 (2020) .
- [9] Viscusi, A., Astarita, A. & Prisco, U. Mechanical properties optimization of friction stir welded lap joints in aluminium alloy. *Advances in Materials Science and Engineering* **2019** (2019) .
- [10] Gutowski, T. *et al.* Environmentally benign manufacturing: observations from japan, europe and the united states. *Journal of Cleaner Production* **13** (1), 1–17 (2005) .
- [11] Dufflou, J., Kellens, K. & Dewulf, W. Unit process impact assessment for discrete part manufacturing: A state of the art. *CIRP Journal of Manufacturing Science and Technology* **4** (2), 129–135 (2011) .
- [12] Ingarao, G. Manufacturing strategies for efficiency in energy and resources use: The role of metal shaping processes. *Journal of Cleaner Production* **142**, 2872–2886 (2017) .
- [13] Lakshminarayanan, A., Balasubramanian, V. & Elangovan, K. Effect of welding processes on tensile properties of aa6061 aluminium alloy joints. *The International Journal of Advanced Manufacturing Technology* **40** (3-4), 286–296 (2009) .
- [14] Bevilacqua, M., Ciarapica, F. E., D’Orazio, A., Forcellese, A. & Simoncini, M. Sustainability analysis of friction stir welding of aa5754 sheets. *Procedia CIRP* **62**, 529–534 (2017). <https://doi.org/https://doi.org/10.1016/j.procir.2016.06.081> .
- [15] Buffa, G. *et al.* An insight into the electrical energy demand of friction stir welding processes: the role of process parameters, material and machine tool architecture. *The International Journal of Advanced Manufacturing Technology* **100** (9), 3013–3024 (2019) .
- [16] Myers, R. H., Montgomery, D. C. & Anderson-Cook, C. M. *Response surface methodology: process and product optimization using designed experiments* (John Wiley & Sons, 2016).
- [17] Wang, Z. *et al.* High temperature deformation behavior of friction stir welded 2024-t4 aluminum alloy sheets. *Journal of Materials Processing Technology* **247** (C), 184–191 (2017). <https://doi.org/10.1016/j.jmatprotec.2017.04.015> .
- [18] Buffa, G., Campanella, D., Di Lorenzo, R., Fratini, L. & Ingarao, G. Analysis of electrical energy demands in friction stir welding of aluminum alloys. *Procedia Engineering* **183**, 206–212 (2017) .